Microchimica Acta (2021) 188: 32
https://doi.org/10.1007/s00604-020-04652-6

ORIGINAL PAPER

Efficient separation of phosphopeptides employing a Ti/Nb-functionalized core-shell structure solid-phase extraction nanosphere

Bin Liu[1] · Baichun Wang[1] · Yinghua Yan[1] · Keqi Tang[1] · Chuan-Fan Ding[1]

Received: 6 July 2020 / Accepted: 17 November 2020 / Published online: 7 January 2021

Abstract

A strategy for effectively enriching global phosphopeptides was successfully developed by using ammonia methyl phosphate (APA) as a novel chelating ligand and Ti^{4+} and Nb^{5+} as double functional ions (referred to as Fe_3O_4@$mSiO_2$@APA@Ti^{4+}/Nb^{5+}). With the advantage of large specific surface area (151.1 m^2/g), preeminent immobilized ability for metal ions (about 8% of total atoms), and unbiased enrichment towards phosphopeptides, Fe_3O_4@$mSiO_2$@APA@Ti^{4+}/Nb^{5+} displays high selectivity (maximum mass ratio β-casein to BSA is 1:1500), low limit of detection (LOD, as low as 0.05 fmol), good relative standard deviation (RSD, lower than 7%), recovery rate of 87% (^{18}O isotope labeling method), outstanding phosphopeptide loading capacity (330 μg/mg), and at least five times re-use abilities. In the examination of the actual sample, 24 phosphopeptides were successfully detected in saliva and 4 phosphopeptides were also selectively extracted from human serum. All experiments have shown that Fe_3O_4@$mSiO_2$@APA@Ti^{4+}/Nb^{5+} exhibits exciting potential in view of the challenge of low abundance of phosphopeptides.

Keywords Phosphopeptides · Enrichment · Metal ion affinity chromatography (IMAC) · MALDI-TOF MS

Introduction

Reversible phosphorylation of proteins is one of the pervasive and paramount post-translational modifications (PTM) [1]. Phosphorylation serves as irreplaceable part in vital movement processes, such as intercellular signaling, transduction, and neural activity [2, 3]. Some physiological abnormalities and pathologies are thought to be associated with abnormal phosphorylation, and some phosphorylated proteins have become biomarkers of several kinds of diseases [4, 5]. Therefore, understanding the reaction mechanism of protein phosphorylation and phosphorylation sites has a non-negligible effect on understanding the life activities of organisms. Mass spectrometry has become an irreplaceable tool in proteomics/polypeptide omics analysis due to its high sensitivity and resolution. However, due to the influence of the phosphoric acid group, the ionization efficiency of phosphopeptides is poorer than that of non-phosphopeptides, and the abundance of phosphopeptides is lower. Therefore, there is considerable impediment to the direct analysis of actual biological samples by mass spectrometry without pretreatment. Various unfavorable factors require us to develop an efficient method for isolating phosphopeptides from complex biological samples [6, 7].

To date, researchers have made much effort to developing strategies for enrichment of phosphopeptides, including immunoprecipitation [8], reverse liquid chromatography [9], ion-exchange chromatography (IEC) [10, 11], and affinity chromatography [12–14]. Affinity chromatography-immobilized metal ion affinity chromatography (IMAC) has become a prevalent strategy due to the simple operation steps along with the diversity of metal cations and chelating ligands [15–21]. The enrichment mechanism is based on a coordination reaction between metal ions and phosphate groups, so the phosphopeptides can be captured under acidic conditions and eluted under alkaline conditions [22]. Therefore, many high-valent metal ions have been explored and used for the phosphorylated protein separation and enrichment, and most of them have achieved good results. Up to

✉ Yinghua Yan
yanyinghua@nbu.edu.cn

[1] Zhejiang Provincial Key Laboratory of Advanced Mass Spectrometry and Molecular Analysis, Institute of Mass Spectrometry, School of Material Science and Chemical Engineering, Ningbo University, Ningbo 315211, Zhejiang, China

now, there are more than 10 types of metal ions that have been developed for phosphopeptide detection, such as Fe^{3+}, Ti^{4+}, Cu^{2+}, Ni^{3+}, Zr^{4+}, Nb^{5+}, Ga^{3+}, and Zn^{2+} [23–27]. Because of the diversity of vacancy orbit and positive charge of metal ions, the affinity of different metal ions to phosphopeptides is different, which affects the analysis of global phosphopeptides [28]. For example, Ti^{4+}, Fe^{3+}, and Tb^{3+} tend to capture monophosphopeptides, while Cu^{2+}, Ni^{3+}, Zr^{4}+, Nb^{5+}, Ga^{3+}, and Zn^{2+} have stronger attraction for multi-phosphopeptides [21]. Therefore, working out a nanocomposite with the capability of enrichment of global phosphopeptides has become a hot spot in the research of phosphorylated proteomics [29].

The selection of chelating ligands is the priority in the study of IMAC materials. In the 1970s, it was observed that cysteine, histidine, and copper ions can form stable complexes in aqueous solutions, and the complexes can enrich some specific proteins in the solution, thus making the application of IMAC method expands to macromolecular protein [30]. In 1986, Andersson further developed this method by combining iminodiacetic acid (IDA) with Fe^{3+} chelation, which made phosphate amino acids in the solution preserved, while the non-phosphate amino acids did not, indicating that IDA could be used as a chelating ligand of metal cations to enrich phosphopeptides [31]. Subsequently, a variety of chelating ligands have been developed, such as NTA, PDA, and ATP, which can not only chelate metal cations but also increase the hydrophilicity of the material, greatly promoting the development of phosphoproteomics [32–34]. For example, Deng research group prepared the material Fe_3O_4@PDA-Ti/Nb by using polydopamine (PDA) as chelating ligand for loading Ti and Nb. Comparing with only one metal ion-loaded material (Fe_3O_4@PDA-Ti and Fe_3O_4@PDA-Nb), Fe_3O_4@PDA-Ti/Nb displayed better enrichment efficiency than the single metal ion-loaded microspheres [35]. This work has contributed a lot to the development of phosphorylated proteomics. Nevertheless, the Fe_3O_4 has relatively low surface area. Therefore, development of new ligands and materials with large specific surface area is still an urgent task.

Herein, a brand-new chelating agent, ammonia methyl phosphate (APA), was developed to immobilize two metal ions Ti^{4+}/Nb^{5+} to the magnetic mesoporous silicon dioxide matrix (denoted as Fe_3O_4@$mSiO_2$@APA@Ti^{4+}/Nb^{5+}). Ti^{4+}/Nb^{5+} endowed the newly prepared nanosphere with the capability to capture global phosphopeptides. Ti^{4+} ion is one of the most commonly used ions in the IMAC method; the maturity of its development and research can ensure that the material has a certain enrichment performance. In addition, after investigation, it is found that Nb^{5+} has an excellent enrichment effect on polyphosphorylated peptides among many metal cations, and can make up for the deficiency of Ti^{4+} ion in the enrichment of polyphosphorylated peptides. The introduction of the new chelating ligand APA made the material excellent metal cation chelating ability, which greatly improves the loading of metal ions for the specific adsorption of phosphorylated peptides. Fe_3O_4@$mSiO_2$ was used as the core, which not only imparts strong magnetism for material separation but also provides excellent water dispersion as well as plenty of loading sites for post-synthesis of the nanosphere. Fe_3O_4@$mSiO_2$@APA@Ti^{4+}/Nb^{5+} with the above merits was anticipated to have great latent capacity in phosphoproteomics study.

Experimental section

Chemicals

Iron chloride hexahydrate ($FeCl_3 \cdot 6H_2O$, AR), dithiothreitol (DTT, AR), ammonium bicarbonate (NH_4HCO_3, AR), iodoacetamide (IAA, AR), hexadecyl trimethyl ammonium bromide (CTAB), sodium hydroxide (NaOH, AR), trifluoroacetic acid (TFA, AR), 3-glycidoxypropyltrimethoxysilane (GLYMO, AR), methylbenzene, and aminomethyl phosphonic acid (APA, AR) were bought from J&K (Shanghai, China, www.jkchemical.com). Albumin from bovine serum (BSA, 98%), ethanol (EtOH, AR), beta-casein (β-casein, 98%), trypsin, DHB, and ethylene glycol were bought from Sigma-Aldrich (www.sigmaaldrich.com). Acetonitrile (ACN, AR), niobium(V) oxalate hydrate ($Nd_2(C_2O_4)_3$, AR), titanic sulfate ($Ti(SO_4)_2$, AR), ammonium hydroxide, and sodium acetate (CH_3COONa, AR) were bought from Aladdin (Shanghai, China, www.aladdin-e.com). Serum and saliva were obtained from affiliated NBU Hospital (number of volunteers: 1, gender: male, age 25).

Preparation of Fe_3O_4@$mSiO_2$@APA@Ti^{4+}/Nb^{5+}

Fe_3O_4 was acquired by the method reported in the previous literature and simply modified [12]. The specific step is to disperse $FeCl_3 \cdot 6H_2O$ (2.7 g) into 150 mL of ethylene glycol ($(CH_2OH)_2$), stirred the mixture through to yellow and transparent (300 rpm/min), after add ground anhydrous sodium acetate (7.2 g) and stir for 2 h (300 rpm/min) that was devolved to a reaction vessel reacted at 200 °C for 16 h. The shell structure $mSiO_2$ was modified by employing a dry magnetic sphere (100 mg) and 1 g of CTAB dispersed in 100 mL deionized water under ultrasound conditions, then, slow accession 10 mM NaOH (100 mL) and 800 mL of deionized water and reacted for 1 h at 60 °C with mechanically stirred (300 rpm/min). Finally, 2 mL of ethanol and 0.5 mL of TEOS were added and mechanically stirred (300 rpm/min) at 60 °C about 12 h, and the obtained products were cleaned three times with water phase (ultrapure water) and organic phase (ethanol). After vacuum dried, the Fe_3O_4@$mSiO_2$ was obtained by calcining dry Fe_3O_4@SiO_2 at 350 °C for 4 h.

Fe_3O_4@$mSiO_2$ (100 mg) was dispersed in 80 mL of toluene solution for ultrasonic dispersion (containing 800 μL of silane coupling agent GLYMO), refluxed at 80 °C for 12 h, cleaned three times with water phase and organic phase and dried under vacuum at 50 °C overnight, and Fe_3O_4@$mSiO_2$-GLYMO was obtained. The chelating ligand APA was immobilized on Fe_3O_4@$mSiO_2$ by a simple synthesis reaction. A total of 100 mg of APA was dispersed in 50 mM NH_4HCO_3 (120 mL) under ultrasonic conditions, then 100 mg of Fe_3O_4@$mSiO_2$-GLYMO was dispersed into 60 mL of the configured APA solution and reacted at 65 °C for 3 h, the supernatant was removed and the remaining APA solution was added, and the reaction was continued for 3 h, washed obtained product, and freeze drying, achieving secondary product Fe_3O_4@$mSiO_2$@APA.

Fe_3O_4@$mSiO_2$@APA@Ti^{4+}/Nb^{5+} was obtained by dispersing Fe_3O_4@$mSiO_2$@APA (200 mg) in 10 mL aqueous solution containing 100 mM Ti $(SO_4)_2$ and 50 mM $Nd_2(C_2O_4)_3$, shaking for 2 h at room temperature and removed supernatant by magnet separation. The obtained final product was cleaned three times with water phase and organic phase, and dried under vacuum at 50 °C for 12 h to obtain Fe_3O_4@$mSiO_2$@APA@Ti^{4+}/Nb^{5+}. Nanosphere of the Fe_3O_4@$mSiO_2$@APA@Ti^{4+} obtained using the same method was almost the same as above except for $Nd_2(C_2O_4)_3$/$Ti(SO_4)_2$.

Characterization

SEM was characterized by a Keol 2012 microscope. X-ray diffraction (XRD) was characterized using Bruker XRD (D4). Infrared (FT-IR) spectroscopy was recorded using Thermo Fisher Scientific 10 infrared spectrometer analysis. Matrix-assisted laser desorption ionization time-of-flight mass spectrometry (MALDI-TOF MS) was used in an autoflex max (Bruker, USA). TEM image was recorded using JEOL 1011 microscopy (Japan), X-ray photoelectron spectroscopy (Axis Ultra DLD), automatic specific surface area, and pore analyzer (HD88, USA Micromeritics).

Standard protein and actual sample pretreatment

β-Casein was primarily pretreated prior to enrichment. A total of 2 mg β-casein was dispersed to 400 μL of ammonium bicarbonate aqueous solution, denatured at 100 °C boiling water for 10 min, after cooling down, enzymatic hydrolysis for 12 h with the help of trypsin (2 mg/mL, 50 μL).

Reduction alkylation of BSA with DTT and IAA was by classic approach. Firstly, 1 mg BSA was dispersed in 200 μL of 50 mM NH_4HCO_3 solution and denatured at 100 °C boiling water for about 10 min. Five microliters 200 mM DTT and 45 μL 50 mM NH_4HCO_3 were added, and shook for 1 h under 37 °C. Next, 10 μL 400 mM IAA and 90 μL 50 mM NH_4HCO_3 were employed of alkylation under the dark of 37 °C about 1 h. Finally, 20 μg of trypsin was added, the final solution was incubated at 37 °C about 16 h.

Saliva comes from healthy adults in the laboratory. Suspended matter in saliva was detached via centrifugation under hypothermia and 14,000 rpm high speed, then, saliva after treatment was used for subsequent experiment. Human serum was used without further treatment.

Enrichment experiment

A total of 500 μg of Fe_3O_4@$mSiO_2$@APA@Ti^{4+}/Nb^{5+} was dispersed into 200 μL of enrichment buffer (ACN/TFA/H_2O = 50%:/0.1%:/49.9%), after ultrasonic for about 5 min, 2 μL of β-casein was appended, removing the supernatant by a magnet after shaken at 37 °C about 30 min, and the phosphopeptide-loaded nanomaterial was washed several times using enrichment buffer (ACN/TFA/H_2O = 50%:/0.1%:/49.9%, about 200 μL). Afterward, incubated for 15 min at 37 °C after 10 μL of desorption buffer ammonia (NH_4OH, 0.4 mol/L) was added. Finally, analysis phosphopeptides from the eluate was by MALDI-TOF MS. The enrichment process of practical samples is the same as above, only changing 2 μL β-casein to 2 μL of practical samples (serum, saliva).

MALDI MS analysis

All detections are carried out in reflected positive ion mode. The instrument uses an improved Nd:YAG laser with a detection frequency of 1000 Hz, a flight tube acceleration voltage of 20 kV, a detector voltage of approximately 18 kV, and detection range of mass charge ratio is 1000–3500 Da. The concentration of matrix DHB is 20 mg/mL, (solvent with ACN/H_2O = 30%/70%).

Results and discussion

Preparation of Fe_3O_4@$mSiO_2$@APA@Ti^{4+}/Nb^{5+} nanosphere

The synthesis process of Fe_3O_4@$mSiO_2$@APA@Ti^{4+}/Nb^{5+} nanosphere was presented in Scheme 1. In short, Fe_3O_4 was first prepared by the hydrothermal method. Next, a mesoporous silica magnetic material Fe_3O_4@$mSiO_2$ was prepared to employ CTAB as the templating agent. Then, the APA chelating agent was successfully modified onto the surface of Fe_3O_4@$mSiO_2$. Finally, Ti^{4+} and Nb^{5+} were modified on APA to prepare Fe_3O_4@$mSiO_2$@APA@Ti^{4+}/Nb^{5+} nanosphere. In order to verify the successful preparation of the material and the performance, we performed a series of characterization and enrichment experiments on the material.

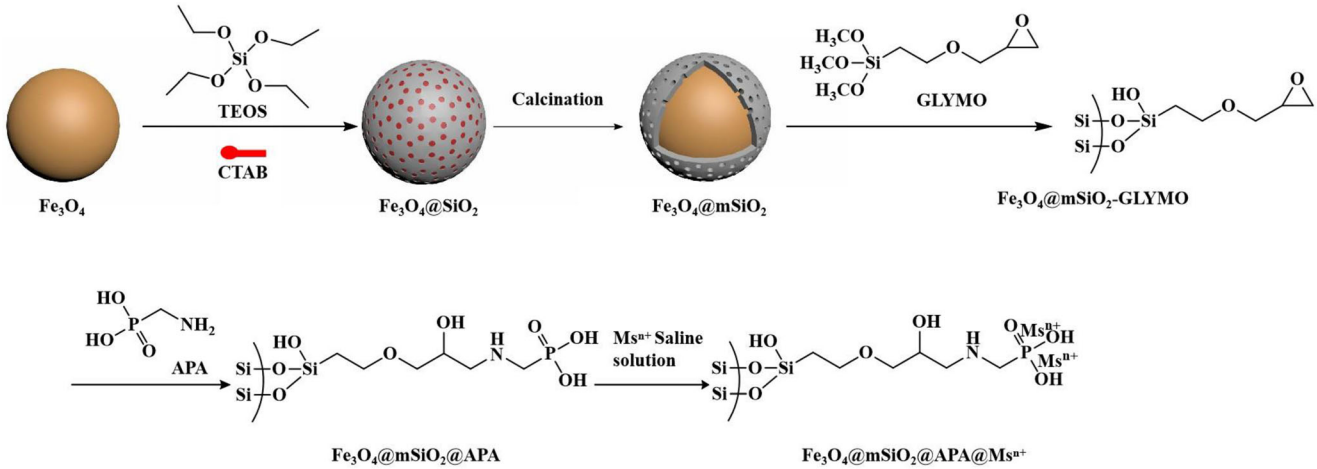

Scheme 1 The preparation step for Fe_3O_4@mSiO$_2$@APA@Ti^{4+}/Nb^{5+}nanosphere

The micromorphic status and particle size of Fe_3O_4@mSiO$_2$@APA@Ti^{4+}/Nb^{5+} were firstly observed through SEM and TEM. As shown in SEM (Fig. 1a, b), the average particle size of the Fe_3O_4@mSiO$_2$@APA@Ti^{4+}/Nb^{5+} is about 200 nm in diameter, and the wrinkles on the surface of the material also indicate that the modifier has been successfully coated on the surface of the material. The TEM image (Fig. 1c, d) shows that the total thickness of silica and other modifications is approximately 30 nm. Ti and Nb observed from EDX analysis show that Ti^{4+} and Nb^{5+} were faultlessly modified onto the material (Fig. S1). XPS analysis was further tested for the elemental composition of the material (Fig. S2). The phase structure of Fe_3O_4@mSiO$_2$@APA@Ti^{4+}/Nb^{5+} was analyzed by XRD ray diffraction. As shown in Fig. S3, the diffraction peaks of 30.1° (220), 43.1° (400), and 57.1° (511) belong to the Fe_3O_4 crystal, and 36.1° (220) and 63.2° (422) belong to the characteristic peak of silicon dioxide. The material was then subjected to Fourier infrared detection to prove successful preparation. Comparing the three curves of Fig. S4, the strong peak at 575 cm^{-1} attributed to the Fe–O, peak at 1100 cm^{-1} belongs to the stretching vibration of Si–O–Si, the infrared peak caused by the stretching vibration of N–H is at 1650 cm^{-1}. It is found in

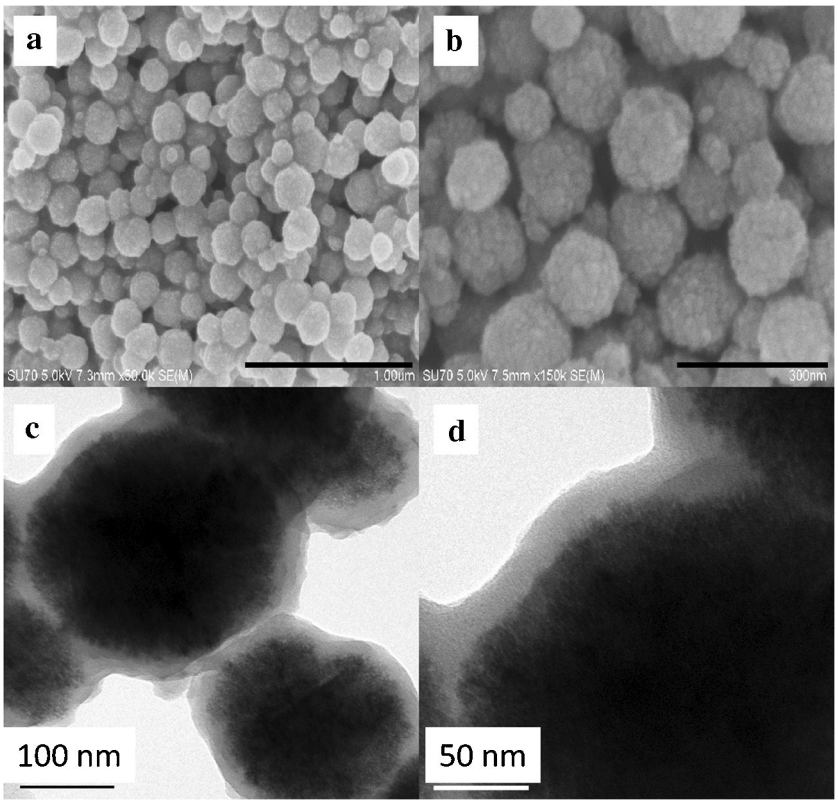

Fig. 1 **a**, **b** SEM image and **c**, **d** TEM image of Fe_3O_4@mSiO$_2$@APA@Ti^{4+}/Nb^{5+}

actual experiments that the nanosphere has excellent water dispersibility as well as an outstanding magnetic response (Fig. S5), which makes the separation of materials extremely simple. Nitrogen adsorption-desorption isotherm indicates the presence of mesoporous channels. As shown in Fig. S6, the BET surface area is 151.1 m^2/g, the total pore volume is 0.17 cm^3/g, and the average pore width (4 V/A by BET) is 4.45 nm. The data shows that Fe_3O_4@$mSiO_2$@APA@Ti^{4+}/Nb^{5+} may have the ability to exclude large volumes of proteins when enriching phosphopeptides.

Investigation on the enrichment of phosphopeptides from β-casein digests

The procedure for enriching phosphopeptides from β-casein digests was displayed in Scheme 2. First of all, Fe_3O_4@$mSiO_2$@APA@Ti^{4+}/Nb^{5+} was dispersed into the loading buffer (ACN/TFA/H_2O = 50%: 0.1%: 49.9%) containing β-casein digest to capture phosphopeptides, then washed several times with loading buffer after enrichment in order to elute the non-phosphopeptides that adhere to the surface of the material. Finally, desorption buffer (0.4 M NH_4OH) was utilized to elute the enriched phosphorylated peptides, and the eluant was analyzed by MALDI-TOF MS.

The enrichment time was firstly investigated under the same conditions except for the enrichment time. The results showed that the two phosphopeptide peaks increased with the increase of enrichment time, but the change range tended to be gentle after 30 min (Fig. S7). Therefore, after comprehensive consideration, we finally selected 30 min as the final enrichment time.

For effective evaluation of the capacity of Fe_3O_4@$mSiO_2$@APA@Ti^{4+}/Nb^{5+} towards phosphopeptides, β-casein was used as a phosphorylated peptide standard protein. Before enrichment, the baseline of the graph was higher and the peak intensity was relatively weak, and no phosphorylated peptides were observed in virtue of the shielding effect of the non-phosphopeptides (Fig. 2a). After enriched with Fe_3O_4@$mSiO_2$@APA@Ti^{4+} (Fig. 2b), 8 phosphopeptides and dephosphopeptides were detected, and the peak strength and the number of hetero-peaks have greatly improved compared to Fig. 2a. Especially, the peak intensity of monophosphopeptides (2061 and 2556) was significantly higher than that of multiphosphopeptides (3122), indicating the enrichment bias of Ti^{4+} to monophosphopeptides. The result enrichment with Fe_3O_4@$mSiO_2$@APA@Nb^{5+} (Fig. 2c) showed Nb^{5+} had a strong affinity for multiphosphopeptides. Figure 2d shows the spectrum obtained after hiring Fe_3O_4@$mSiO_2$@APA@Ti^{4+}/Nb^{5+}, and the typical 2062, 2556, and 3122 phosphopeptides displayed extremely high peak intensity contrast to the precursor material, revealing that the introduction of Ti^{4+} and Nb^{5+} dual ions prominently improved the enrichment efficiency towards global phosphopeptides (the detail information was shown in Table S1). Besides, we also observed the cycle stability of the prepared nanosphere, as shown in Fig. S8, both Fe_3O_4@$mSiO_2$@APA@Ti^{4+} and Fe_3O_4@$mSiO_2$@APA@Ti^{4+}/Nb^{5+} showed good reusability. We also investigated the stability of the material by comparing the performance of the material in different periods (Fig. S9). It can be seen that even if the material was stored for 6 months, it still has good enrichment capacity, which exhibits that the material has a good storage lifetime.

To investigate the effect of Ti/Nb ions on the enrichment of phosphopeptides, enrichment experiments on precursor were carried out and the results were shown in Fig. S10. It was found that the precursor materials had almost no enrichment effect on the phosphopeptides, which indicates that Ti(IV) and Nb(V) ions play a decisive role in the enrichment of phosphopeptides and their amounts have a direct impact on the enrichment performance. Then, three kinds of low concentration solutions of the β-casein were employed to investigate the enrichment LOD of Fe_3O_4@$mSiO_2$@APA@Ti^{4+}/Nb^{5+} (standard is based on the signal-to-noise ratio SNR = 3, and the RSD was lower than 7%, Table S2). As shown in Fig. 3, Fe_3O_4@$mSiO_2$@APA@Ti^{4+} and Fe_3O_4@$mSiO_2$@APA@Ti^{4+}/Nb^{5+} can still enrich

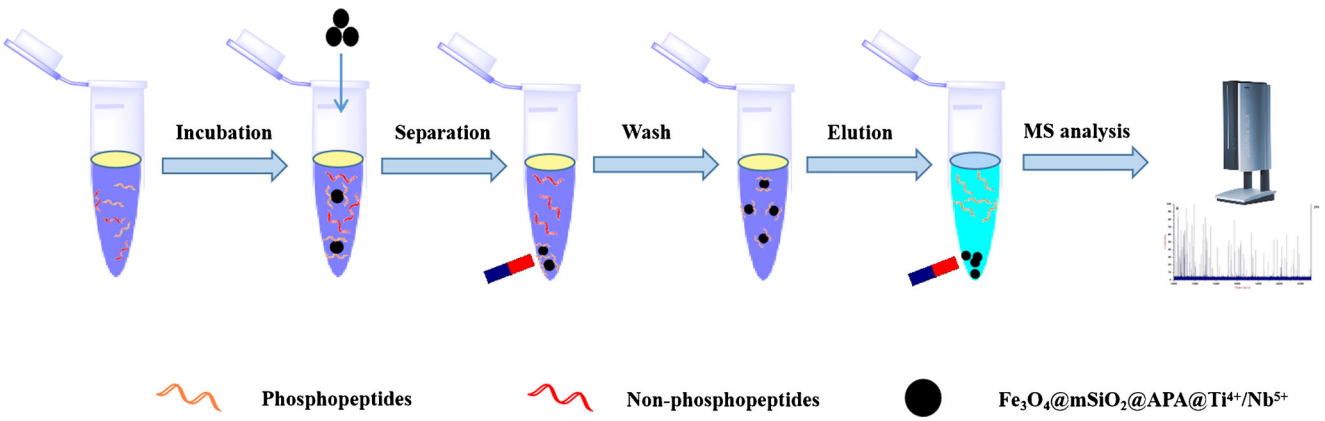

Scheme 2 The preparation step for Fe_3O_4@$mSiO_2$@APA@Ti^{4+}/Nb^{5+}

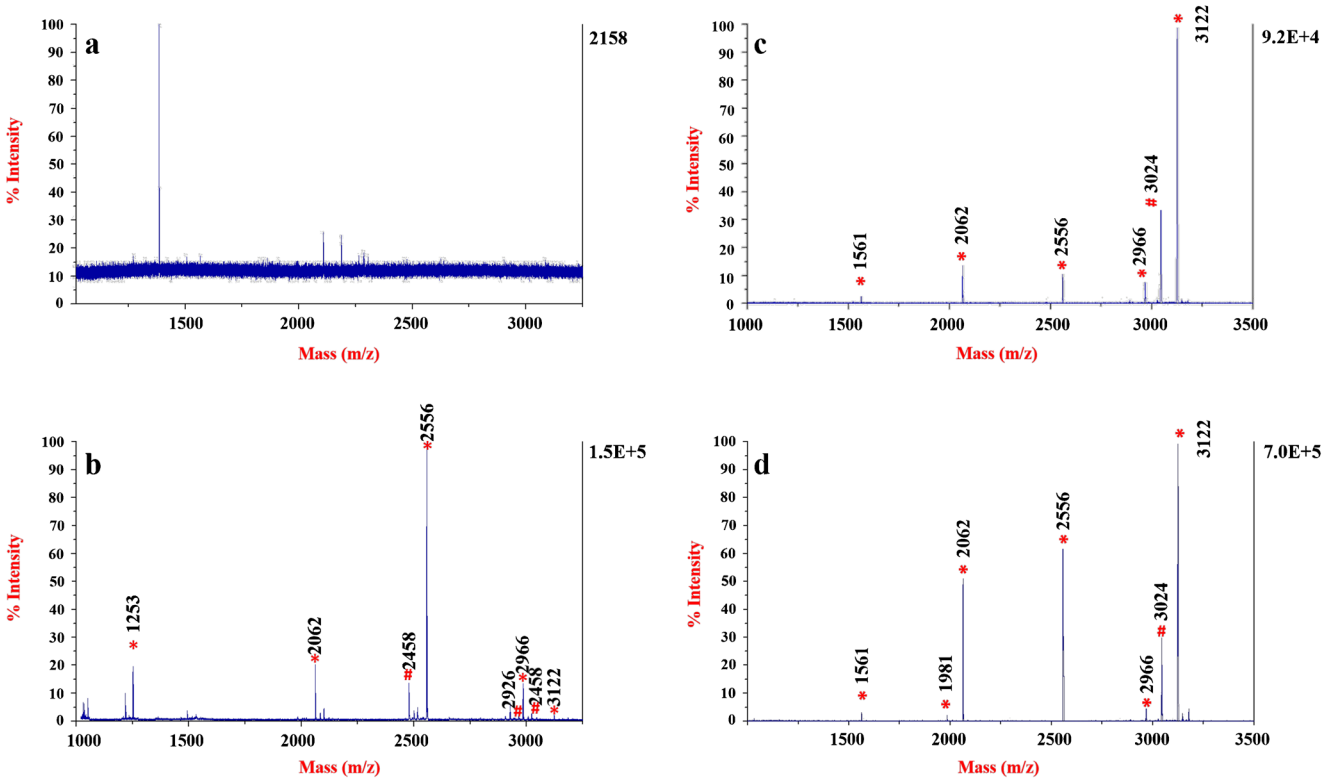

Fig. 2 MALDI-TOF mass spectra of β-casein digests (0.1 pmol).Before enrichment (**a**). Afterenriched with Fe_3O_4@$mSiO_2$@APA@Ti^{4+}(**b**), Fe_3O_4@$mSiO_2$@APA@Nb^{5+}(**c**), and Fe_3O_4@$mSiO_2$@APA@Ti^{4+}/Nb^{5+}(**d**). Phosphopeptide peaks areflagged as "*", dephosphorylated peaks are flagged as"#"

phosphopeptides when the dilution of β-casein was as low as 1 fmol, and when the standard protein β-casein was diluted to 0.5 fmol, only three phosphorylated peptides could be enriched by Fe_3O_4@$mSiO_2$@APA@Ti^{4+}, and the multiphosphopeptide 3122 failed to be enriched. Nevertheless, comparing with the mass spectrum after enrichment by Fe_3O_4@$mSiO_2$@APA@Ti^{4+}/Nb^{5+}, the three typical phosphopeptide peaks are all enriched with higher S/N and peak intensity. Further diluting the standard protein concentration to 0.05 fmol, three phosphorylated peptides can still be enriched by Fe_3O_4@$mSiO_2$@APA@Ti^{4+}/Nb^{5+}, but Fe_3O_4@$mSiO_2$@APA@Ti^{4+} cannot (Fig. S11). It displayed that the immobilization of dual ions improved material both global phosphopeptide affinity and trace detection capability. The above results showed that our new prepared nanosphere Fe_3O_4@$mSiO_2$@APA@Ti^{4+}/Nb^{5+} had a low detection limit for phosphopeptides, which was conducive to the detection of low-level phosphopeptides in actual complex samples. The loading capacity of the Fe_3O_4@$mSiO_2$@APA@Ti^{4+}/Nb^{5+} was investigated by introducing different amounts of the nanosphere into 10 μL β-casein digest. After enrichment, the eluant was detected by MALDI at the same detection conditions.

The capacity of the Fe_3O_4@$mSiO_2$@APA@Ti^{4+}/Nb^{5+} was estimated by observing changes of peak intensity of the three typical phosphopeptides. As shown in Fig. 4, the load capacity of phosphopeptides on Fe_3O_4@$mSiO_2$@APA@Ti^{4+} was increased from 150 to 200 μg, and reached adsorption saturation at 200 μg; the saturation load capacity was calculated to be 333 μg/mg. The maximum load capacity of Fe_3O_4@$mSiO_2$@APA@Ti^{4+}/Nb^{5+} was calculated to be 500 μg/mg using the same method.

The anti-interference performance of the material was detected by adding a certain ratio of BSA digest to the β-casein digest. It can be seen from Fig. 5 and Fig. S12 that both materials have strong anti-interference ability. However, under the same ratio, the dual-ion material enriches more phosphorylated peptides than the single-ion material, further expanding the ratio to 1:1500 and four phosphorylated peptides were still detected after being enriched by Fe_3O_4@$mSiO_2$@APA@Ti^{4+}/Nb^{5+} (Fig. S13). In addition, we directly analyzed the mixture of β-casein:BSA = 1:100 by mass spectrometry without material enrichment, and the results showed that no phosphorylated peptides were detected (Fig. S14). It shows that the introduction of Nb^{5+} ion strengthens the affinity of phosphopeptides, and enhances the specificity towards phosphopeptides. The experimental results showed that Fe_3O_4@$mSiO_2$@APA@Ti^{4+}/Nb^{5+} had excellent enrichment performance on phosphopeptides.

Subsequently, we added the size-exclusion experiment by unhydrolyzed BSA to the hydrolyzed β-casein. The mixed solution was enriched by Fe_3O_4@$mSiO_2$@APA@Ti^{4+}/Nb^{5+}; both the eluent and the supernatant were analyzed by

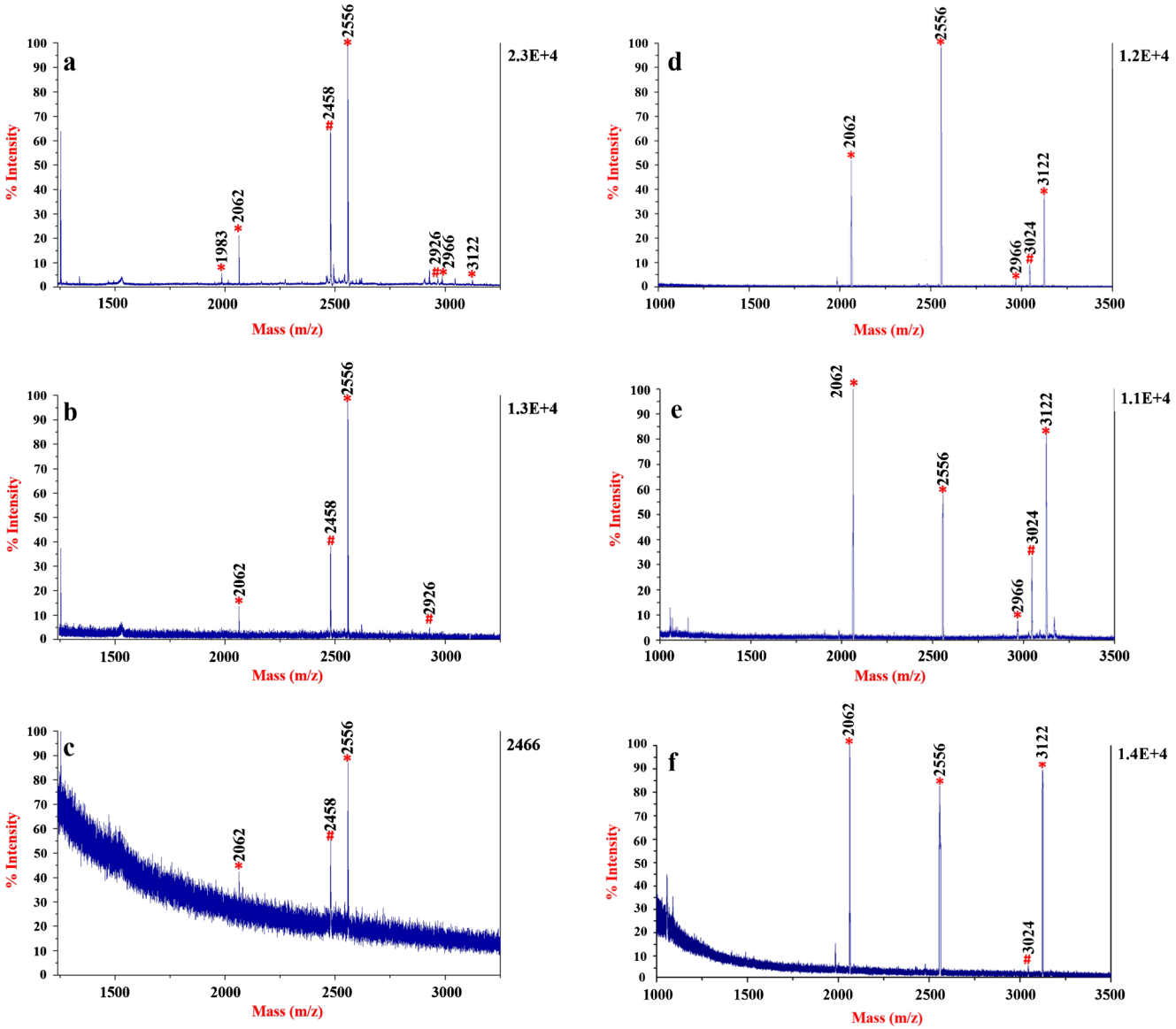

Fig. 3 MALDI-TOF mass spectra analysis of phosphopeptidesfrom weak solutions of the β-casein digests after enriched by 10 fmol (**a**), 1 fmol (**b**), and 0.5 fmol (**c**)Fe_3O_4@$mSiO_2$@APA@Ti^{4+}, and by 10 fmol(**d**), 1 fmol (**e**), and 0.5 fmol (**f**) Fe_3O_4@$mSiO_2$@APA@Ti^{4+}/Nb^{5+}.Phosphopeptide peaks are flagged as "*", dephosphorylated peaks are flaggedas"#"

mass spectrometry. As shown in Fig. S15, the phosphopeptide peak was only observed in the elution, and there was no signal of BSA intact protein, and BSA protein peak was observed in the supernatant. The above results showed that the material Fe_3O_4@$mSiO_2$@APA@Ti^{4+}/Nb^{5+} had a significant size exclusion effect on bulk materials.

The enrichment recovery rate of Fe_3O_4@$mSiO_2$@APA@Ti^{4+}/Nb^{5+} on the phosphopeptides was detected by the isotope labeling method. In short, β-casein was treated with trypsin in $H_2{}^{16}O$ and $H_2{}^{18}O$ to obtain ^{16}O- and ^{18}O-labeled β-casein digests, which produced a mass difference of 4 Da in mass spectrometry (introducing two ^{18}O atoms). Take two equal amounts of the digests with heavy label and light label. Firstly, the light label β-casein fraction was enriched with materials, and the eluent was mixed with the heavy label fraction, and the mixture materials were enriched with Fe_3O_4@$mSiO_2$@APA@Ti^{4+}/Nb^{5+}. The eluent was analyzed by mass spectrometry. The recovery of the material was obtained by calculating the ratio of the peak intensity of the lightly isotope-labeled phosphopeptide to the peak intensity of the corresponding heavy isotope-labeled phosphopeptide. After repeating the experiment three times, the average recovery rate of the material is 87% (Fig. S16).

Study enrichment of biological samples

Actual samples of human serum and saliva were hired to examine whether the material can be used to analyze complex samples

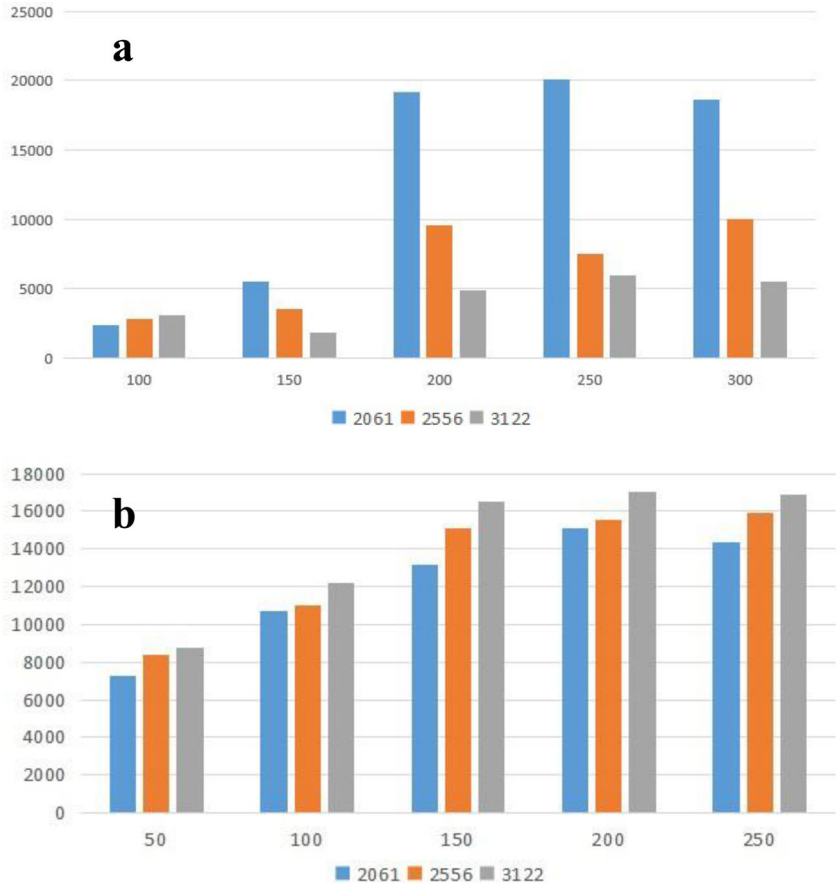

Fig. 4 Calculation of the loading capacity forphosphopeptides. Fe_3O_4@$mSiO_2$@APA@Ti^{4+}(**a**). Fe_3O_4@$mSiO_2$@APA@Ti^{4+}/Nb^{5+}(**b**)

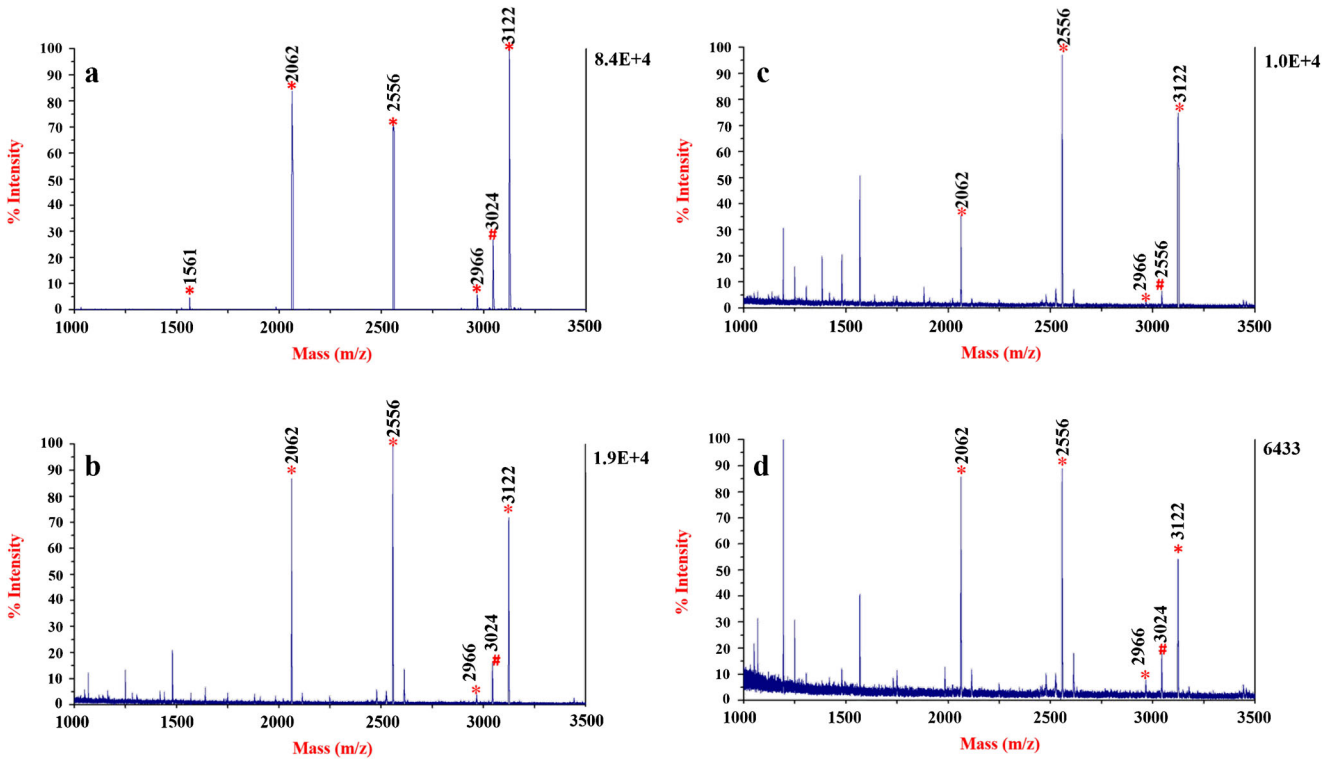

Fig. 5 MALDI-TOF mass spectra of enriched phosphopeptidesfrom a mixture of β-casein and BSA with a mass ratio of 1:100 (**a**), 1:250 (**b**), 1:500 (**c**), and 1:1000(**d**) with Fe_3O4@$mSiO_2$@APA@Ti^{4+}/Nb^{5+}.Phosphopeptide peaks are flagged as "*", dephosphorylated peaks are flaggedas"#"

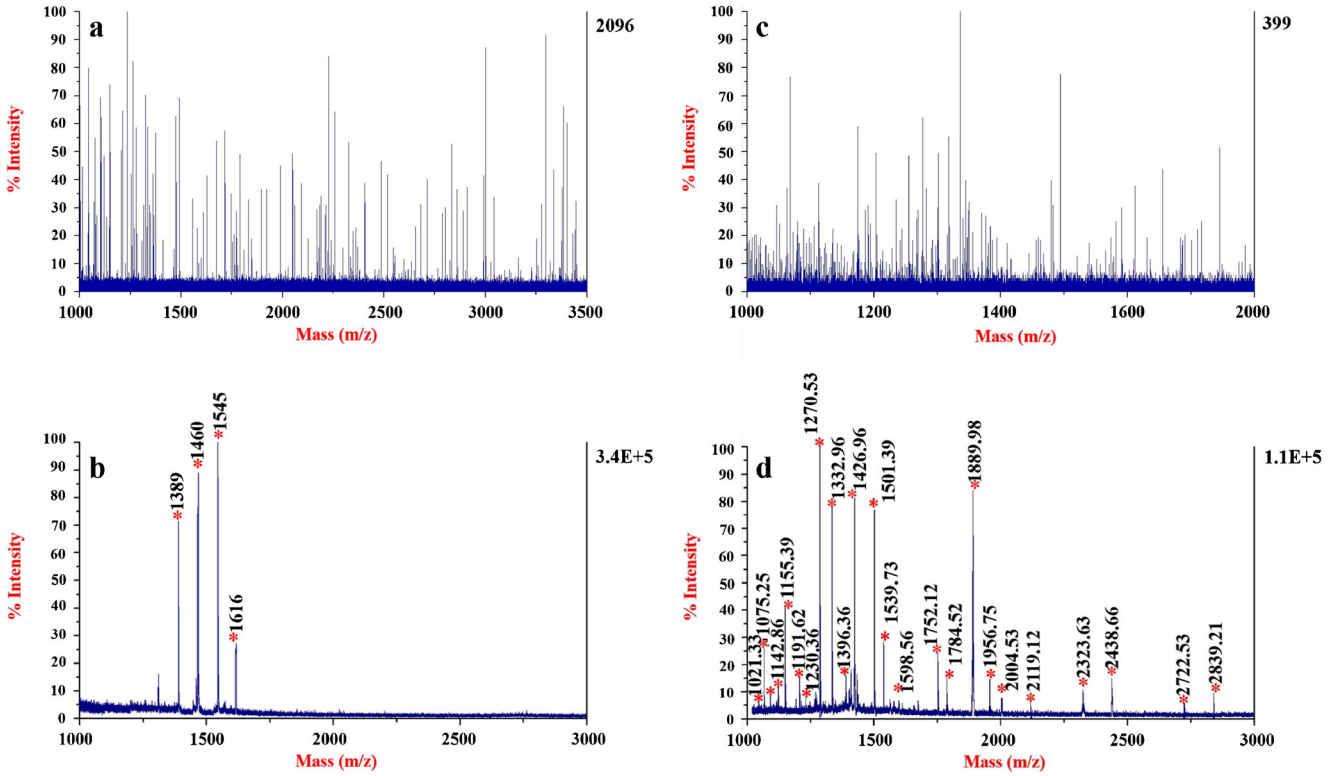

Fig. 6 MALDI-TOF mass spectra of phosphopeptides from humanserum: before enrichment (**a**), afterenrichment by Fe_3O_4@$mSiO_2$@APA@Ti^{4+}/Nb^{5+}(**b**), mass spectra of phosphopeptidesfrom saliva: before enrichment (**c**), afterenrichment by Fe_3O_4@$mSiO_2$@APA@Ti^{4+}/Nb^{5+}(**d**). Phosphopeptide peaks areflagged as "*"

(Fig. 6). Four phosphopeptide peaks were detected from human serum (Table S3) and 24 phosphopeptides were analyzed in the saliva treated with Fe_3O_4@$mSiO_2$@APA@Ti^{4+}/Nb^{5+}. The above results indicated that Fe_3O_4@$mSiO_2$@APA@Ti^{4+}/Nb^{5+} nanomaterial had surprising application value in actual research. Based on the perfect chelation of metal ions and phosphate groups, we believe the compounds containing phosphate and carboxyl groups can be exacted using our prepared material. In addition, in order to prove the excellent enrichment efficiency of Fe_3O_4@$mSiO_2$@APA@Ti^{4+}/Nb^{5+} materials, we selected several Ti^{4+} IMAC nano-adsorbed materials previously reported; comparing with the other materials in Table 1, Fe_3O_4@$mSiO_2$@APA@Ti^{4+}/Nb^{5+} is superior in selectivity and detection limits.

Conclusions

Based on the IMAC enrichment strategy, we successfully developed a novel material for phosphopeptide enrichment by a

Table 1 Enrichment efficiency comparison with previously reported materials

Materials	LOD	Selectivity	Actual sample	Numbers	
MCNC@COF@Zr^{4+}	10 fmol	BSA:β-casein = 200:1	Serum	4	[23]
TpPA-2-Ti^{4+}	4 fmol	BSA:β-casein = 100:1	Non-fat milk	12	[36]
MG@$mSiO_2$-ATP-Ti^{4+}	4 fmol	BSA:β-casein = 100:1	Serum and saliva	4, 19	[33]
MCNC@PMAA@PEG@Ti^{4+}	50 fmol	BSA:β-casein = 500:1	Serum	4	[29]
EGMP@Ti^{4+}	5 fmol	BSA:β-casein = 500:1	Rat liver digests	216	[37]
MagSiO_2@SIO_2@PDA@Ti^{4+}	50 fmol	BSA:β-casein = 500:1	Serum	4	[38]
Fe_3O_4@PDA-Ti/Nb	2 fmol	BSA:β-casein = 1000:1	Serum	4	[35]
Fe_3O_4@PDA@Zr-Ti-MOF	0.4 fmol	BSA:β-casein = 1000:1	Saliva	25	[20]
Ti^{4+}@Zr-MOF	1 fmol	BSA:β-casein = 80:1	Saliva	24	[39]
MagG@PDA@Ni-MOF@Fe-MOF	4 fmol	BSA:β-casein = 1000:1	Saliva	24	[40]
Fe_3O_4@$mSiO_2$@APA@Ti^{4+}/Nb^{5+}	0.05 fmol	BSA:β-casein = 1500:1	Serum and saliva	4, 24	This work

simple synthesis method. Fe_3O_4@$mSiO_2$@APA@Ti^{4+}/Nb^{5+} nanosphere greatly improves the characteristics of single metal ion IMAC material biased to phosphopeptide; this material enhances the affinity of IMAC nanomaterials for global phosphopeptides. The employment of the brand-new chelating agent APA enormously ameliorates the immobilization efficiency of metal ions, so that the enriched phosphopeptides has a higher signal. Although Fe_3O_4@$mSiO_2$@APA@Ti^{4+}/Nb^{5+} has good selectivity and specificity towards phosphopeptides, the material still has some limitations, for example, the surface area is relatively small, and there are many synthetic steps.

Supplementary Information The online version contains supplementary material available at https://doi.org/10.1007/s00604-020-04652-6.

Funding This work is supported by Zhejiang Natural Science Foundation (LQ19C050002), State Key Laboratory of Analytical Chemistry for Life Science (SKLACLS1901), National Natural Science Foundation of China (511903050), and the K. C. Wong Magna Fund in Ningbo University.

Compliance with ethical standards

Conflict of interest The authors declare that they have no competing interests.

References

1. Wu YL, Liu QJ, Deng CH (2019) L-Cysteine-modified metal-organic frameworks as multifunctional probes for efficient identification of N-linked glycopeptides and phosphopeptides in human crystalline lens. Anal Chim Acta 1061:110–121
2. Wang ZD, Wang JW, Sun NR, Deng CH (2019) A promising nanoprobe based on hydrophilic interaction liquid chromatography and immobilized metal affinity chromatography for capture of glycopeptides and phosphopeptides. Anal Chim Acta 1067:1–10
3. Wang JW, Wang ZD, Sun NR, Deng CH (2019) Immobilization of titanium dioxide/ions on magnetic microspheres for enhanced recognition and extraction of mono- and multi-phosphopeptides. Microchim Acta 186:236
4. Sun NR, Wang ZD, Wang JW, Chen HM, Wu H, Shen S, Deng CH (2019) Hydrophilic tripeptide combined with magnetic titania as a multipurpose platform for universal enrichment of phospho- and glycopeptides. J Chromatogr A 1595:1–10
5. Sun NR, Wang JW, Yao JZ, Chen HM, Deng CH (2019) Magnetite nanoparticles coated with mercaptosuccinic acid-modified mesoporous titania as a hydrophilic sorbent for glycopeptides and phosphopeptides prior to their quantitation by LC-MS/MS. Microchim Acta 186:159
6. Li YL, Liu LL, Wu H, Deng CH (2019) Magnetic mesoporous silica nanocomposites with binary metal oxides core-shell structure for the selective enrichment of endogenous phosphopeptides from human saliva. Anal Chim Acta 1079:111–119
7. Wu YL, Liu QJ, Xie YQ, Deng CH (2018) Core-shell structured magnetic metal-organic framework composites for highly selective enrichment of endogenous N-linked glycopeptides and phosphopeptides. Talanta 190:298–312
8. Zheng HY, Hu P, Quinn DF, Wang YK (2005) Phosphotyrosine proteomic study of interferon alpha signaling pathway using a combination of immunoprecipitation and immobilized metal affinity chromatography. Mol Cell Proteomics 4:721–730
9. Faserl K, Kremser L, Muller M, Teis D, Lindner HH (2015) Quantitative proteomics using ultralow flow capillary electrophoresis-mass spectrometry. Anal Chem 87:4633–4640
10. Hennrich ML, Groenewold V, Kops GJ, Heck AJ, Mohammed S (2011) Improving depth in phosphoproteomics by using a strong cation exchange-weak anion exchange-reversed phase multidimensional separation approach. Anal Chem 83:7137–7143
11. Atakay M, Celikbicak O, Salih B (2012) Amine-functionalized sol-gel-based lab-in-a-pipet-tip approach for the fast enrichment and specific purification of phosphopeptides in MALDI-MS applications. Anal Chem 84:2713–2720
12. Cao LC, Zhao YM, Chu ZY, Zhang XM, Zhang WB (2020) Core-shell magnetic bimetallic MOF material for synergistic enrichment of phosphopeptides. Talanta 206:120165
13. Xiao RL, Pan YN, Li J, Zhang LY, Zhang WB (2019) Layer-by-layer assembled magnetic bimetallic metal-organic framework composite for global phosphopeptide enrichment. J Chromatogr A 1601:45–52
14. Jiang DD, Li XQ, Jia Q (2018) Design of two-dimensional layered double hydroxide nanosheets embedded with Fe_3O_4 for highly selective enrichment and isotope labeling of phosphopeptides. ACS Sustain Chem Eng 7:421–429
15. Xiao J, Yang SH, Wu JX, Wang H, Yu X, Shang WB, Chen GQ, Gu ZY Highly selective capture of monophosphopeptides by two-dimensional metal-organic framework nanosheets. Anal Chem 91: 9093–9101
16. Jiang DD, Li Z, Jia QA (2019) Sensitive and selective phosphopeptide enrichment strategy by combining polyoxometalates and cysteamine hydrochloride-modified chitosan through layer-by-layer assembly. Anal Chim Acta 1066:58–68
17. Ma WF, Zhang Y, Li LL, You LJ, Zhang P, Zhang YT, Li JM, Yu M, Guo J, Lu HJ, Wang CC (2012) Tailor-made magnetic Fe_3O_4@$mTiO_2$ microspheres with a tunable mesoporous anatase shell for highly selective and effective enrichment of phosphopeptides. ACS Nano 6:3179–3188
18. Lin HZ, Chen HM, Shao X, Deng CH (2018) A capillary column packed with a zirconium (IV)-based organic framework for enrichment of endogenous phosphopeptides. Microchim Acta 185:562
19. Lu J, Qi DW, Deng CH, Zhang XM, Yang PY (2010) Hydrothermal synthesis of alpha-Fe_2O_3@SnO_2 core-shell nanotubes for highly selective enrichment of phosphopeptides for mass spectrometry analysis. Nanoscale 2:1892–1900
20. Liu QJ, Sun NR, Gao MX, Deng CH (2018) Magnetic binary metal–organic framework as a novel affinity probe for highly selective capture of endogenous phosphopeptides. ACS Sustain Chem Eng 6:4382–4389
21. Jiang JB, Sun XN, Li Y, Deng CH, Duan GL (2018) Facile synthesis of Fe_3O_4@PDA core-shell microspheres functionalized with various metal ions: a systematic comparison of commonly-used metal ions for IMAC enrichment. Talanta 178:600–607
22. Cho KY, Chen LJ, Hu YW, Schnaubelt M, Zhang H (2019) Developing workflow for simultaneous analyses of phosphopeptides and glycopeptides. ACS Chem Biol 14:58–66
23. Gao CH, Bai J, He YT, Zheng Q, Ma WD, Lei ZX, Zhang MY, Wu J, Fu FF, Lin Z (2019) Postsynthetic functionalization of Zr^{4+}-immobilized core-shell structured magnetic covalent organic frameworks for selective enrichment of phosphopeptides. ACS Appl Mater Interfaces 11:13735–13741
24. Bae SW, Kim JI, Cuot I, Sung J, Hong JI, Yeo WS (2017) Zinc ion-immobilized magnetic microspheres for enrichment and identification of multi-phosphorylated peptides by mass spectrometry. Anal Sci 33:1381–1386

25. Lai AC, Tsai CF, Hsu CC, Sun YN, Chen YJ (2012) Complementary Fe^{3+} and Ti^{4+}-immobilized metal ion affinity chromatography for purification of acidic and basic phosphopeptides. Rapid Commun Mass Sp 26:2186–2194
26. Matthew C, Paul T (2012) Immobilized gallium (III) affinity chromatography of phosphopeptides. Anal Chem 71:2883–2892
27. Alexander L, Martin S, Wolfgang L (2011) Tools for analyzing the phosphoproteome and other phosphorylated biomolecules: a review. Anal Chim Acta 703:19–30
28. Zhai R, Tian F, Xue RQ, Jiao FL, Hao FR, Zhang YJ, Qian XH (2016) Metal ion-immobilized magnetic nanoparticles for global enrichment and identification of phosphopeptides by mass spectrometry. RSC Adv 6:1670–1677
29. Ma WF, Zhang Y, Li LL, Zhang YT, Yu M, Guo J, L HJ, Wang C (2013) Ti^{4+}-immobilized magnetic composite microspheres for highly selective enrichment of phosphopeptides. Adv Funct Mater 23:107–115
30. Porath J, Carlsson J, Olsson I, Belfrage G (1975) Metal chelate affinity chromatography, a new approach to protein fractionation. Nature 258:598–599
31. Andersson L, Porath J (1986) Isolation of phosphoproteins by immobilized metal (Fe^{3+}) affinity chromatography. Anal Biochem 154:250–254
32. Ficarro SB, Adeimant G, Tomar MN, Zhang Y, Cheng VJ, Marto JA (2009) Magnetic bead processor for rapid evaluation and optimization of parameters for phosphopeptide enrichment. Anal Chem 81:4566–4575
33. Yan YH, Zheng ZF, Deng CH, Zhan XM, Yang PY (2013) Facile synthesis Ti^{4+}-immobilized Fe_3O_4@polydopamine core-shell microspheres for highly selective enrichment of phosphopeptides. Chem Commun 49:5055–5057
34. Su J, He XW, Chen LX, Zhang YK (2018) Adenosine phosphate functionalized magnetic mesoporous graphene oxide nanocomposite for highly selective enrichment of phosphopeptides. ACS Sustain Chem Eng 6:2188–2196
35. Jiang JB, Sun XN, She XJ, Li JJ, Li Y, Deng CH, Duan G (2018) Magnetic microspheres modified with Ti(IV) and Nb(V) for enrichment of phosphopeptides. Microchim Acta 185:309–316
36. Wang HP, Jiao FL, Gao FY, Lv YY, Wu Q, Zhao Y, Shen YH, Zhang YJ, Qian XH (2017) Titanium (IV) ion-modified covalent organic frameworks for specific enrichment of phosphopeptides. Talanta 166:133–140
37. Zhou HJ, Ye ML, Dong J, Han GH, Jiang XN, Wu RN, Zou HF (2008) Specific phosphopeptide enrichment with immobilized titanium ion affinity chromatography adsorbent for phosphoproteome. Analysis 7:3957–3967
38. Salimi K, Usta DD, Celikbicak O, Pinar A, Salih B, Tuncel A (2017) Ti (IV) carrying polydopamine-coated, monodisperse-porous SiO_2 microspheres with stable magnetic properties for highly selective enrichment of phosphopeptides. Colloids Surf B: Biointerfaces 153:280–290
39. Zheng HY, Wang JX, Gao MX, Zhang XM (2019) Titanium (IV)-functionalized zirconium-organic frameworks as dual-metal affinity probe for recognition of endogenous phosphopeptides prior to mass spectrometric quantification. Microchim Acta 186:829–839
40. Wang BC, Liu B, Yan YH, Tang KQ, Ding CF (2019) Binary magnetic metal-organic frameworks composites: a promising affinity probe for highly selective and rapid enrichment of mono- and multi-phosphopeptides. Microchim Acta 186:832–841